Tetrahedron 65 (2009) 9460–9467

Contents lists available at ScienceDirect

Tetrahedron

journal homepage: www.elsevier.com/locate/tet

# Calamitic metallomesogens derived from unsymmetric pyrazoles

Min-Chou Chen [c], Shih-Chieh Lee [c], Chia-Chung Ho [a], Tarng-Shiang Hu [a], Gene-Hsiang Lee [b], Chung K. Lai [c,*]

[a] Industrial Technology Research Institute, HsinChu 300, Taiwan, ROC
[b] Instrumentation Center, National Taiwan University, Taipei 10660, Taiwan, ROC
[c] Department of Chemistry, National Central University, Chung-Li 32001, Taiwan, ROC

ARTICLE INFO

*Article history:*
Received 11 July 2009
Received in revised form 19 August 2009
Accepted 25 August 2009
Available online 29 August 2009

ABSTRACT

Three series of copper(II) complexes **1a**–**1c** derived from unsymmetric pyrazoles **2a**–**2c** were prepared and their mesomorphic properties investigated. The mesomorphic behavior of compounds was studied by differential scanning calorimetry, polarizing optical microscopy, and powder X-ray diffractometry. The crystal and molecular structures of mesogenic copper complex (**2a**; $n$=10) of 3-[4-decyloxyphenyl]-1*H*-pyrazole were determined by means of X-ray structural analysis. It crystallizes in the triclinic space group *P*-1, with $a$=4.0890(1) Å, $b$=18.0167(2) Å, $c$=25.5015(5) Å, and $Z$=2. The geometry at copper center was not perfectly square planar. A weak intermolecular H-bond ($d$=2.36 Å) between Cl1 and H2 atoms and π–π interaction (ca. 3.45–3.55 Å) was also observed. All their precursors **2a**–**2c** were not mesogenic. In contrast, copper complexes **1a** formed nematic or smectic C phases and complexes **1b**–**1c** formed crystalline phases. Powder X-ray diffraction experiments confirmed the presence of SmC phase.



## 1. Introduction

Pyrazoles,[1] classified as heterocyclic compounds, and their metal pyrazolate[2] have been widely applied in inorganic, organometallic, and bioinorganic chemistry. As with most other heterocyclic compounds they are often considered as electron-deficient or electron acceptors, therefore, a local dipole of donor-to-acceptor (D–A) interaction was possibly induced within molecules or between molecules. This type of weak intermolecular interaction was often applied to generate useful materials with preferred molecular orientation in a particular state. Liquid crystalline material is such an example. In addition, intramolecular or intermolecular hydrogen bondings (–NH···N) can be also possibly induced in such systems if molecules designed properly. In fact hydrogen bonded liquid crystals[3] or H-bond-stabilized LCs have been widely observed in mesogenic materials, as well as in a few pyrazole derivatives.[4] X-ray crystallographic analysis indicated that H-bonds can be either intermolecularly[3c] or/and intra-molecularly induced. Interest in such systems stems from their diverse structures and known chemistry. More and more examples of mesogenic pyrazoles[4] were reported since the first symmetric mesogenic pyrazoles[5] **Ia** prepared and investigated in 1992. On the other hand, two nitrogen atoms on the pyrazole ring are potentially capable of binding to metal ions. Their possible structures can be various and diverse. A trinuclear Au(I) pyrazole-based complex[6] bearing long alkyl chains has been prepared and its solution in hexane was found to form a red-luminescent organogel ($\lambda_{em}$=640, $\lambda_{ext}$=284 nm) for an application of reversible RGB color switching. In contrast, known metallomesogens derived from pyrazoles were relatively scarce, some of the complexes incorporated with Ir/Rh(I/II),[7] Ni(II),[8] and Pd(II),[9] Cu(I/II),[10] Ag/Au(I),[11] and Zn(II)[12] ions were already reported. Columnar or smectic phases were obtained by rhodium(I) complexes derived from symmetrical or unsymmetric pyrazoles. A few novel samples of trimetallomesogens constructed by use of Ag(I) and Au(I) with a coordination number equal to two were also prepared, and columnar phases observed. On the other hand, mesogenic Pd(II) and Ni(II) complexes were also obtained by symmetric or unsymmetrical pyrazole. The geometry at metal center was mostly square planar or distorted tetrahedral. Metallomesogens with a square planar geometry often facilitated the molecular arrangements in solid or LC states. These reported mesogens or metallomesogens formed layer smectic or columnar phases. Some of structurally similar symmetrical **Ib** or unsymmetric pyrazoles[13] **II**–**IV** and their derived metallomesogens **V**,[10] **VI**[8] were previously prepared in this group.

Here we wish to report the preparation, characterization, and mesomorphic studies of three series of rod-like copper(II) complexes **1a**–**1c** derived from unsymmetric pyrazoles **2a**–**2c**. The crystal and molecular structures of mesogenic copper complex (**1a**; $n$=10) of 3-[4-decyloxyphenyl]-1*H*-pyrazole were determined by means of X-ray structural analysis, and geometry at copper center was perfectly square planar. All pyrazoles **2a**–**2c** were not

* Corresponding author.
*E-mail address:* cklai@cc.ncu.edu.tw (C.K. Lai).

0040-4020/$ – see front matter © 2009 Elsevier Ltd. All rights reserved.
doi:10.1016/j.tet.2009.08.062

mesogenic. Copper complexes **1a** formed nematic or smectic phases, however, copper complexes **1b**–**1c** were not mesogenic. The preferred mesophase formation of compound **1a** over **1b**–**1c** might probably be attributed to a better aspect ratio. XRD experiments were also performed to confirm the presence of SmC phase. EPR studies indicated the presence of anisotropic behavior at paramagnetic copper(II) center. The relationship between molecular structures and mesomorphic behavior was also discussed. This is the second example of copper pyrazolate complexes exhibiting mesomorphic behavior.

of pyrazoles **2a**–**2c** with copper(II) chloride in refluxing THF/$C_2H_5OH$ produced the copper complexes **1a**–**1c** as bright yellowish green solids. The similar reactions with $ZnCl_2$ to prepare zinc complexes were not successful for an unknown reason. Similar palladium(II) complexes[9e–g] has been prepared and studied.

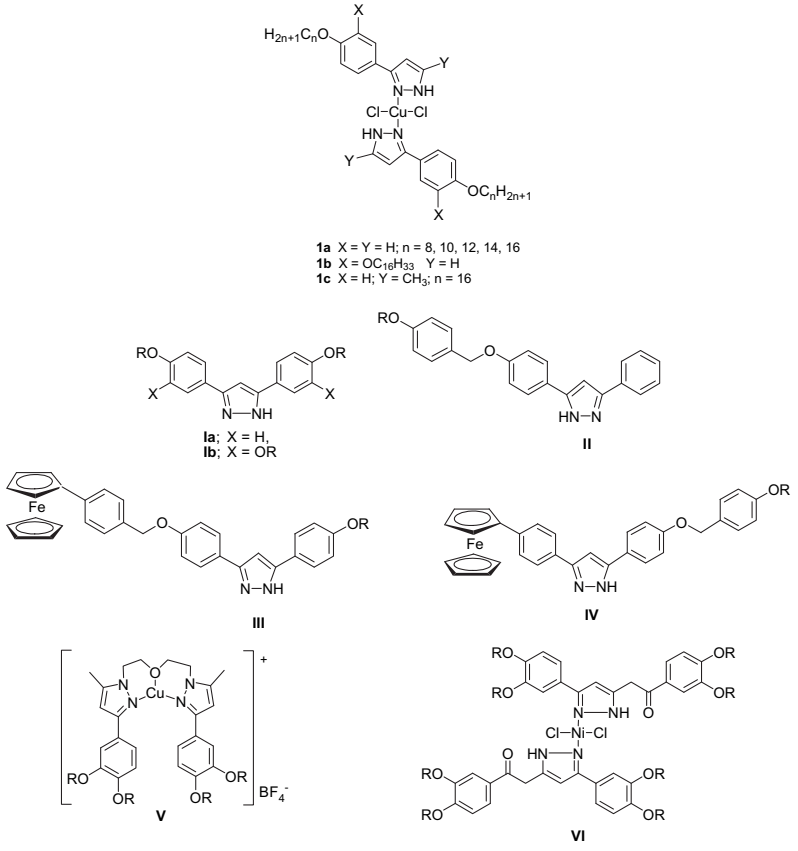


## 2. Results and discussion

### 2.1. Synthesis and characterization

The synthetic pathways[14] followed to prepare compounds **1a**–**1c** are summarized in Schemes 1 and 2. All precursors **3a**–**3c** were prepared according to the literature procedures. The further condensation reactions of 1-(4-alkoxyphenyl)-3-hydroxy-2-propen-1-ones **3a**, 1-(3,4-alkoxy phenyl)-3-hydroxy-2-propen-1-ones **3b**, and 4-hexadecoxyphenylbutane-1,3-dione **3c** with hydrazine monohydrate in refluxing absolute ethanol produced the pyrazole derivatives **2a**–**2c** as off-white solids with a yield of ca. 61–83%. All compounds were characterized by $^1H$ and $^{13}C$ NMR spectroscopy. The formation for compound **2c** was easily monitored by the disappearance of a singlet at $\delta$ 16.30 assigned for –CHCO*H* of **3c** on $^1H$ NMR spectroscopy. Similarly, the formation for compound **2a** was also monitored by the disappearance of a singlet at $\delta$ 9.93–8.11 assigned for –CO*H* of **3a** on $^1H$ NMR spectroscopy. Two tautomers for pyrazoles **2a**–**2b** are spectroscopically observed. On the $^1H$ NMR spectra, only two characteristic peaks at $\delta$ 6.50–6.55 and 7.57–7.63, assigned to keto-H(–C*H*CN) pyrazole-H(=C*H*NH) were observed, however, the pyrazole-H(–N*H*) often occurred at $\delta$ 11.60–12.60 was not observed. The further reactions

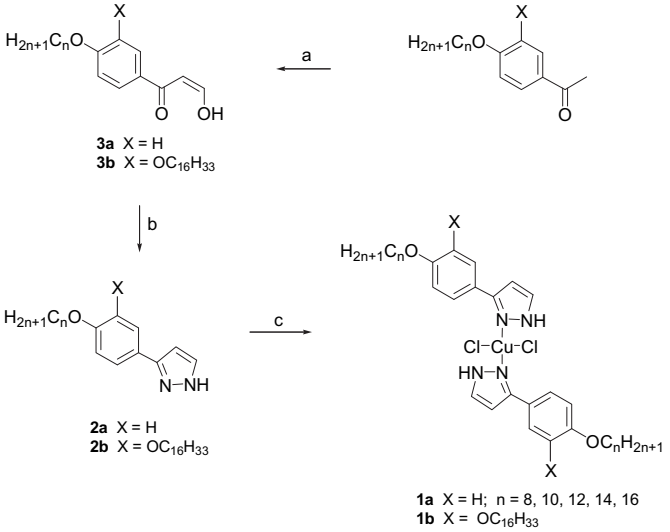


**Scheme 1.** Reagents and conditions. (a) NaOMe, ethyl formate, stirring at rt in dry THF, 24 h. (b) Hydrazine monohydrate, refluxing in THF/$C_2H_5OH$, 24 h. (c)$CuCl_2$, refluxing in THF/$C_2H_5OH$, 1 h.

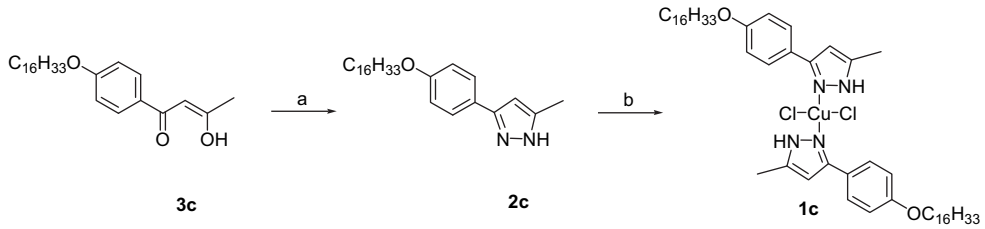


**Scheme 2.** Reagents and conditions. (a) Hydrazine monohydrate, refluxing in THF/$C_2H_5OH$, 24 h. (b) $CuCl_2$, refluxing in THF/$C_2H_5OH$, 1 h.

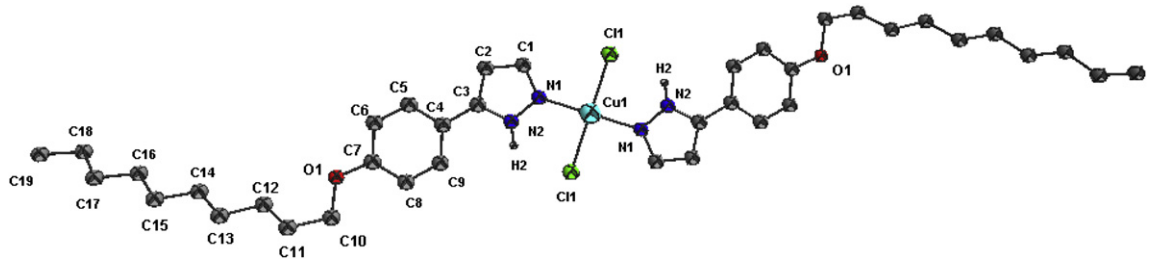


**Figure 1.** An ORTEP drawing for **1a** ($n$=10) with the numbering scheme. The thermal ellipsoids of the non-hydrogen atoms are drawn at the 50% probability level.

## 2.2. X-ray crystallographic analysis of copper complex of 3-[4-decyloxyphenyl]-1*H*-pyrazole (1a; *n*=10)

A needle-like single crystal **1a** ($n$ = 10) grown slowly from $CH_2Cl_2$ solution suitable for X-ray crystallography was obtained by diffusion technique at room temperature and the structure resolved. The molecular structure with numbering scheme is shown in Figure 1. Table 1 lists its crystallographic and structural refinement data for the molecule. The unit cell is triclinic and the molecular geometry is fully extended with two molecules per unit cell. The overall molecular shape is considered as a nearly linear structure, and the molecular length (C19–C19′ atoms) and width were measured as ~40.59 Å and ~4.41 Å, respectively, resulting in a rod-like molecule with an aspect ratio of ~0.11 (4.41/40.59 Å). The geometry at copper center was perfectly square planar, and copper atom was *trans*-coordinated to the two chlorine atoms. The two angles of N(1)–Cu–Cl(1A) and N(1)–Cu–N(2) were of 90.09° and 89.91°, which were close to an ideal angle of 90° expected for a square planar geometry. Two bond distances of Cu–N(1) and Cu–Cl(1) were 1.9815(1) Å and 2.3093(5) Å. Two chlorines, two nitrogens, and copper atom were in fact coplanar, however, this defined plane was not coplanar with the neighboring pyrazole ring, having a dihedral angle of ~9.96°. On the

**Table 1**
Crystal and refinement data for compound **1a** ($n$=10)

| | |
|---|---|
| Compound | **1a** ($n$=10) |
| Empirical formula | $C_{38}H_{56}Cl_2CuN_4O_2$ |
| Formula weight | 735.31 |
| Temperature | 200(2) K |
| Wavelength | 0.71073 Å |
| Crystal system | Triclinic |
| Space group | *P*-1 |
| *a*/Å | 4.0890(1) |
| *b*/Å | 18.0167(3) |
| *c*/Å | 25.5015(5) |
| *α*/° | 89.925(1) |
| *β*/° | 88.968(1) |
| *γ*/° | 84.413(1) |
| *U*/Å$^3$ | 1869.47(7) |
| *Z* | 2 |
| $D_c$/Mg/m$^3$ | 1.306 |
| *F*(000) | 782 |
| Crystal size/mm$^{-3}$ | 0.35×0.15×0.12 |
| Reflections collected | 18,944 |
| Independent reflections | 8543 [$R_{(int)}$=0.0338] |
| Data/restraints/parameters | 8543/0/429 |
| Final *R*1, *wR*2 | 0.0382, 0.1110 |

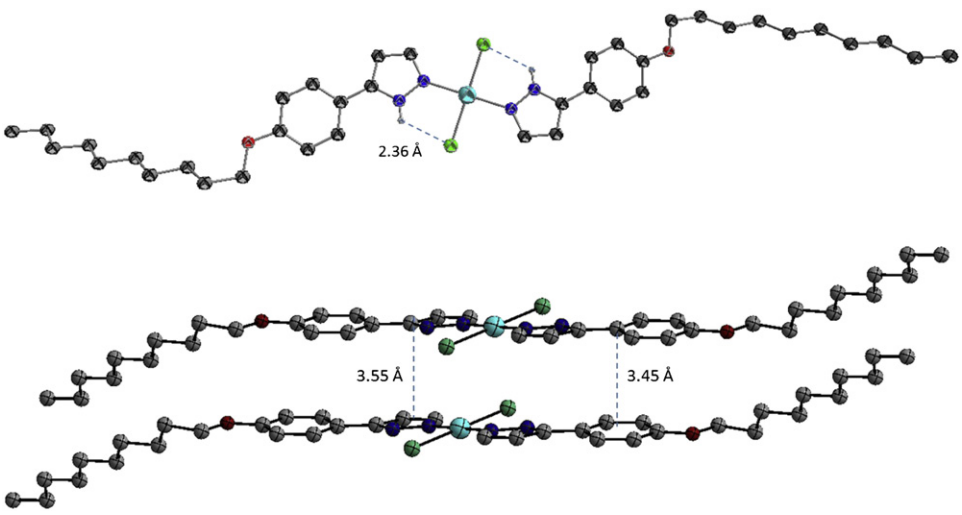


**Figure 2.** A weak intramolecular H-bond (~2.36 Å) and an π–π interaction (~3.45 Å) were observed in crystal **1a** ($n$=10).

other hand, both pyrazole and benzene rings were also not coplanar with a dihedral angle of ~6.63°. Surprisingly, a weak intramolecular H-bond (~2.36 Å) between Cu atom and the H(2) of the pyrazole ring and π–π interaction (~3.45 Å) are observed in crystal **1a** ($n$=10), shown in Figure 2. This H-bonding kept two chlorines, copper, and two pyrazole rings nearly coplanar, which probably better facilitated the molecular packing both in the solid and/or liquid crystalline state. However, no intermolecular H-bonding was observed. Some selected bond distances and angles for compound **1a** ($n$=10) are summarized in Table 2. A view of the crystal packing in the unit cell is presented in Figure 3 and reveals that the molecules were all tilted by ca. ~53° within the layers. This was quite consistent for the SmC phases observed. All terminal alkoxy chains were in fact interdigitated, and arranged parallel to each other in an extended fashion.

**Table 2**
Selected bond distances and angles in crystal **1a** ($n$=10)

| | | | |
|---|---|---|---|
| *Bond distances* | | | |
| Cu–N(1) | 1.9815(18) | Cu–Cl(1) | 2.3093(5) |
| N1(1)–N(2) | 1.356(3) | N(1)–C(1) | 1.329(3) |
| N(2)–C(3) | 1.349(3) | C(1)–C(2) | 1.386(3) |
| C(2)–C(3) | 1.371(3) | | |
| *Bond angles* | | | |
| N(1)–Cu–N(1A) | 180.00(15) | Cl(1)–Cu–Cl(1A) | 180.00(3) |
| N(1)–Cu–Cl(1A) | 90.09(6) | Cl(1)–Cu–Cl(1A) | 180.00(3) |
| N(2)–N(1)–Cu | 121.98(14) | C(1)–N(1)–Cu | 133.07(17) |
| C(1)–N(1)–N(2) | 104.86(18) | C(3)–N(2)–N(1) | 112.58(19) |
| N(1)–C(1)–C(2) | 110.4(2) | N(2)–C(3)–C(2) | 105.2(2) |
| C(3)–C(2)–C(1) | 107.0(2) | | |

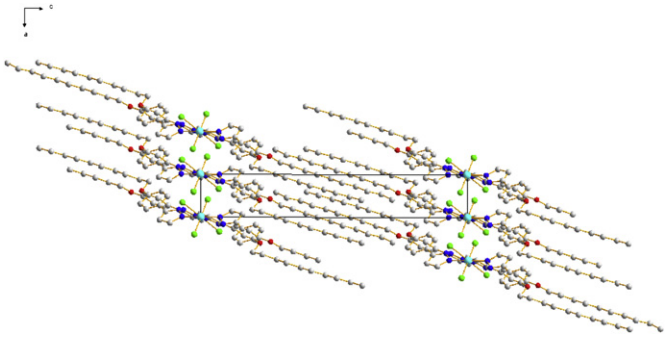

**Figure 3.** Molecular arrangements viewed from $b$ axis in the unit cell.

## 2.3. Mesomorphic properties

The thermal behavior of compounds **1a**–**1c** and **2a**–**2c** were investigated by polarized optical microscopy (POM) and differential scanning calorimetry (DSC). The transition temperatures and enthalpies of the compounds are listed in Table 3. All pyrazole derivatives **2a**, **2b** were not mesogenic. A transition of crystal-to-isotropic was observed at 89.5 °C and 80.6 °C, respectively, for compound **2a** ($n$=12) and **2b** ($n$=16) on heating process. A slightly

**Table 3**
The transition temperatures[a] and enthalpies of compounds **1**–**2**

| | | | | | | | | |
|---|---|---|---|---|---|---|---|---|
| **2a**; n = 12 | | | | | | Cr | 89.5 (45.3) / 63.1 (44.9) | I |
| **2b**; n = 16 | $Cr_1$ | 57.6 (27.4) / 49.0 (50.0) | $Cr_2$ | 60.8 (-43.6) | $Cr_3$ | | 80.6 (55.0) | I |
| **2c**; n = 16 | | | $Cr_1$ | 30.2 (2.52) / 80.0 (57.8) | $Cr_2$ | | 101.0 (58.1) | I |
| **1a**; n = 8 | $Cr_1$ | 92.7 (29.2) / 34.3 (21.0) | $Cr_2$ | 120.9 (29.1) / 108.3 (30.2) | N | | 124.6 (1.32) / 121.5 (3.68) | I |
| 10 | | | Cr | 122.0 (26.6) / 108.4 (26.1) | SmC | | 130.1 (10.7) / 125.8 (11.0) | I |
| 12 | $Cr_1$ | 104.6 (9.72) / 106.9 (19.6) | $Cr_2$ | 122.8 (20.4) | SmC | | 137.7 (10.0) / 130.0 (9.71) | I |
| 14 | $Cr_1$ | 106.1 (27.4) / 105.2 (27.4) | $Cr_2$ | 114.7 (19.1) | SmC | | 136.1 (14.9) / 133.6 (13.6) | I |
| 16 | $Cr_1$ | 72.8 (69.9) | $Cr_2$ | 113.3 (99.9) / 101.3 (20.5) | SmC | | 138.5 (12.7) / 131.5 (12.3) | I |
| **1b**; n = 16 | | | $Cr_1$ | 106.8 (11.8) / 119.8 (43.6) | $Cr_2$ | | 125.7 (44.5) | I |
| **1c**; n = 16 | $Cr_1$ | 74.1 (8.39) / 50.4 (23.9) | $Cr_2$ | 84.4 (1.43) / 78.7 (1.00) | $Cr_3$ | | 108.7 (40.2) | I |

[a] $n$=The carbon numbers in the alkoxy chains, Cr=crystal, N=nematic, SmC=smectic C, I=isotropic phase. The phase transition temperatures (°C) and enthalpies (in parentheses, kJ/mol) were determined by DSC at a scan rate of 10 °C/min.

bent shape and more lath-like shape generated by **2a** and **2b**, respectively, might be attributed to the lack of mesophase. A similar compound **2c** ($n$=16) with one methyl group added on the terminal core moiety did not improve the mesophase, and a higher clearing temperature at $T_{cl}$=101.0 °C was only observed. The same structural effect on the formation of mesophases induced by the presence of a terminal methyl group extended to the core has been previously observed in other metallomesogens.[15] On the other hand, the mesomorphic properties were better improved upon complexation to copper ion. All compounds **1a** with two alkoxy chains displayed enantiotropic liquid crystalline behavior, however, other compounds **1b** with four alkoxy chains formed crystalline phase. The clearing temperatures of copper complexes **1a**–**1c** were all higher than those of their precursor compounds **2a**–**2c**, which were attributed to the larger molecular size or/and core rigidity. They exhibited nematic or smectic C phases, as expected for rod-like and linear molecules. These mesophases were identified by polarized optical microscope. Compound **1a** ($n$=8) with shorter terminal alkoxy chains formed N phase, whereas, all other compounds **1a** with longer terminal alkoxy chains ($n$=10, 12, 14, 16) formed SmC phase. A nematic schlieren texture (Fig. 4) with homeotropic domains under polarizing microscopy was observed when cooled from isotropic liquid. The phases of compounds **1a** ($n$=10, 12, 14, 16) were identified as smectic C phases, and typical textures described as schlieren domains (Fig. 4) were easily observed under optical polarized microscope when cooling from isotropic liquid. The preferred formation of SmC phase over N phase in rod-like mesogens appended with longer terminal chains was attributed to the stronger van der Waals interaction. These textures were not homeotropic, which were often observed in SmA phases. A reasonable enthalpy (i.e., $\Delta H$=10.7–14.9 kJ/mol on heating cycle) for the transition of SmC→I phase was obtained. On heating they all showed only one transition from mesophase-to-isotropic, however, a few extra transitions of crystal-to-crystal were also observed in this system. The clearing temperatures slightly increased with carbon length of terminal alkoxy chains, i.e., $T_{cl}$=138.5 °C ($n$=16)>137.7 °C ($n$=12)>124.6 °C ($n$=8). The temperature range of mesophase also increased with carbon length, i.e., $\Delta T$=30.2 °C ($n$=16)>23.1 °C ($n$=12)>13.2 °C ($n$=8) on cooling process. Both compounds **1b** and **1c** were also not mesogenic as their ligands **2b** and **2c**. Trying to improve the formation of mesophase by adding a methyl group on the core in compound **1c** was in fact unsuccessful. A tetrahedral methyl group might have increased the interlayer distances, thus destroying the mesophase.

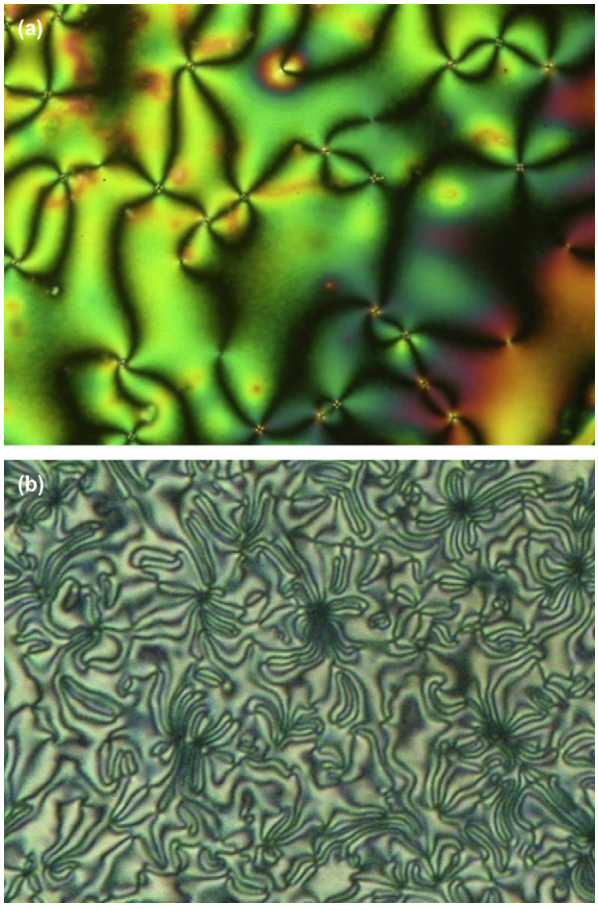


**Figure 4.** The optical textures. (a) Top plate: nematic phase observed by **1a** ($n$=8) at 118 °C and (b) bottom plate: smectic C phase observed by **1a** ($n$=10) at 120.0 °C.

### 2.4. XRD diffraction data and EPR study

Variable-temperature powder XRD experiments were conducted to confirm the structure of the mesophases. For compound **1a** ($n$=10) measured at 126.0 °C one strong diffraction peak and a relatively weak peak at lower angle was observed, shown in Figure 5. These two diffraction peaks corresponded to a layer structure of SmC phase with a spacing of $d_{001}$ ~42.34 Å and $d_{002}$ ~21.13 Å. The observed $d$-spacing was slightly longer than that of molecular length (~40.59 Å) obtained from single crystallographic data. This implied that the molecules were probably not interdigitated between the molten alkoxy chains in the mesophase. Also a very road diffuse halo peak (~4.45 Å) at wide-angle region was observed.

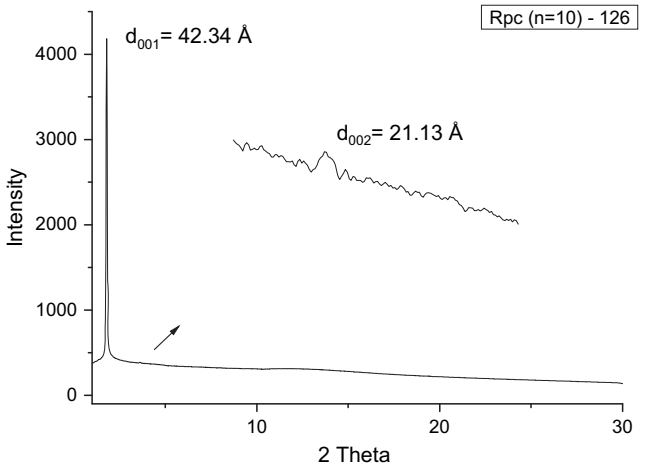


**Figure 5.** The XRD diffraction plot for compound **1a** ($n$=10) measured at 126.0 °C.

Electron paramagnetic resonance spectroscopy has been a valuable technique for investigating the mesomorphic behavior of paramagnetic metallomesogenic materials.[16] Figure 6 shows the X-band EPR spectra of copper complex **1a** ($n$=10) measured at 77 K and at 298 K. Two spectra were only slightly different in peak shape, which might be attributed to preferred molecular orientation or arrangement at two lower temperatures. The spectra consist of broad lines, not expected as a resolved three-line hyperfine band ($^{63.5}$Cu, $I$=1/2) of the characteristic $d^9$-$Cu^{2+}$ center and the hyperfine structure was not observed. The spectra consist of two features, one shoulder barely observed in the low-field region and the other in the high-field region. The lack of the hyperfine structures was probably due to the strong exchange interaction among the paramagnetic copper centers. The EPR data also indicated that the spectra were independent of the aliphatic chain length. However, more useful spectrum measured at mesophase temperature was not possible due to the instrument's limitation.

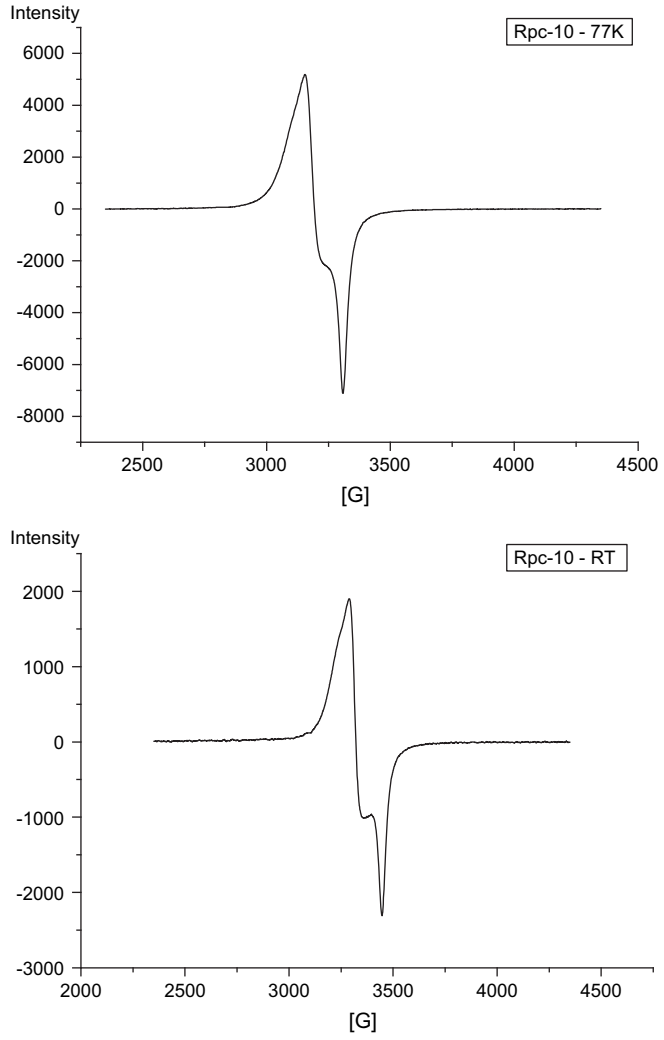


**Figure 6.** The EPR spectra of copper complex **1a** ($n$=10) measured at 77 K (top) and at 298 K (bottom).

## 3. Conclusions

A new series of rod-like metallomesogens exhibiting nematic or smectic phases was prepared and studied. X-ray single crystallographic results indicated that the geometry at copper center was perfectly square planar. These copper complexes **1a** exhibited N or SmC phase. A methyl group added close to rigid core increased the interlayer distances, hence losing liquid crystallinity.

## 4. Experimental

### 4.1. General

All chemicals and solvents were reagent grade from Aldrich Chemical Co., and all solvents were dried by standard techniques. $^1$H and $^{13}$C NMR spectra were measured on a Bruker DRS-200. DSC thermographs were carried out on a Mettler DSC 822 and calibrated with a pure indium sample. All phase transitions are determined by a scan rate of 10.0 °/min. Optical polarized microscopy was carried out on Zeiss Axioplan 2 equipped with a hot stage system of Mettler FP90/FP82HT. Elemental analyses were performed on a Heraeus CHN-O-Rapid elemental analyzer. The powder diffraction data were collected from the Wiggler-A beam line of the National Synchrotron Radiation Research Center (NSRRC) with the wavelength of 1.3263 Å. The powder samples were charged in Lindemann capillary tubes (80 mm long and 0.01 mm thick) from Charles Supper Co. with an inner diameter of 1.0 mm.

### 4.2. 4-Dodecyloxyacetophenone ($n$=12)

White solids. $^1$H NMR (300 MHz, $CDCl_3$): $\delta$ 0.86 (t, 3H, –$CH_3$, $J$=6.5 Hz), 1.18–1.63 (m, 18H, –$CH_2$), 1.73–1.82 (m, 2H, –$CH_2$), 3.99 (t, 2H, –$OCH_2$, $J$=6.6 Hz), 6.88 (d, 4H, Ar–H, $J$=8.7 Hz), 7.89 (d, 4, Ar–H H, $J$=8.7 Hz). $^{13}$C NMR (75 MHz, $CDCl_3$): $\delta$ 14.09, 22.67, 25.95, 26.29, 29.08, 29.33, 29.56, 29.62, 31.90, 68.25, 114.11, 130.09, 130.55, 163.12, 196.74.

### 4.3. 1-(4-Dodecyloxyphenyl)-3-hydroxy-2-propen-1-one (3a; $n$=12)

The solution of 4-dodecyloxyacetophenone (3.00 g, 9.85 mmol) dissolved in 30 mL of THF and NaOMe (0.74 g, 14.78 mmol) was stirred for 30 min. To the solution was dropwise added ethyl formate (0.95 g, 12.81 mmol). The solution was stirred at room temperature for 24 h to give yellow cloudy solution of sodium salts. The solids were filtered, and the solution was extracted with $H_2O$/$CH_2Cl_2$ (1/1). The organic layers were then collected and dried over $NaSO_4$. The solution was concentrated to give yellow solids. The product isolated as light yellow solids were obtained after recrystallization from THF. Yield 72%. $^1$H NMR (300 MHz, $CDCl_3$): $\delta$ 0.86 (t, 3H, –$CH_3$, $J$=6.52 Hz), 1.24–1.82 (m, 20H, –$CH_2$), 3.99 (t, 2H, –$OCH_2$, $J$=6.46 Hz), 6.12 (d, 1H, CH, $J$=4.47 Hz), 6.91 (d, 2H, Ar–H, $J$=8.72 Hz), 7.85 (d, 2H, Ar–H, $J$=8.80 Hz), 8.10 (d, 1H, –COCH, $J$=3.65 Hz), 9.93 (s, 1H, –COH). $^{13}$C NMR (75 MHz, $CDCl_3$): $\delta$ 14.05, 22.63, 25.91, 29.03, 29.29, 29.50, 29.52, 29.58, 31.86, 68.25, 97.62, 114.41, 127.37, 129.53, 130.76, 163.16, 176.46, 188.09.

### 4.4. 1-(4-Octyloxyphenyl)-3-hydroxy-2-propen-1-one (3a; $n$=8)

Light yellow solids. $^1$H NMR (300 MHz, $CDCl_3$): $\delta$ 0.85 (t, 3H, –$CH_3$, $J$=6.00 Hz), 1.24–1.81 (m, 12H, –$CH_2$), 3.98 (t, 2H, –$OCH_2$, $J$=6.60 Hz), 6.12 (d, 1H, –COHCH, $J$=4.40 Hz), 6.90 (d, 2H, Ar–H, $J$=7.04 Hz), 7.84 (d, 2H, Ar–H, $J$=7.04 Hz), 8.10 (d, 1H, –(CO)CH, $J$=4.44 Hz), 9.93 (s, 1H, –COH). $^{13}$C NMR (75 MHz, $CDCl_3$): $\delta$ 14.04, 22.60, 25.93, 29.04, 29.16, 29.26, 31.75, 68.18, 68.27, 68.35, 97.65, 114.34, 114.43, 129.56, 163.18, 176.50, 188.11.

### 4.5. 1-(4-Decyloxyphenyl)-3-hydroxy-2-propen-1-one (3a; $n$=10)

Light yellow solids. $^1$H NMR (300 MHz, $CDCl_3$): $\delta$ 0.85 (t, 3H, –$CH_3$, $J$=6.00 Hz), 1.25–1.83 (m, 16H, –$CH_2$), 3.99 (t, 2H, –$OCH_2$, $J$=6.54 Hz), 6.13 (d, 1H, CH, $J$=4.47 Hz), 6.91 (d, 2H, Ar–H, $J$=8.98 Hz), 7.85 (d, 2H, Ar–H, $J$=8.95 Hz), 8.11 (d, 1H, –COCH, $J$=4.47 Hz), 9.93 (s, 1H, –COH). $^{13}$C NMR (75 MHz, $CDCl_3$): $\delta$ 14.07, 22.64, 25.94, 29.06, 29.28, 29.31, 29.51, 31.86, 68.29, 97.66, 114.00, 114.44, 127.41, 129.56, 130.80, 163.19, 176.50, 188.13.

### 4.6. 1-(4-Tetradecyloxyphenyl)-3-hydroxy-2-propen-1-one (3a; $n$=14)

Light yellow solids. $^1$H NMR (300 MHz, $CDCl_3$): $\delta$ 0.86 (t, 3H, –$CH_3$, $J$=6.58 Hz), 1.24–1.83 (m, 24H, –$CH_2$), 3.99 (t, 2H, –$OCH_2$, $J$=6.60 Hz), 6.13 (d, 1H, CH, $J$=4.50 Hz), 6.91 (d, 2H, Ar–H, $J$=8.80 Hz), 7.85 (d, 2H, Ar–H, $J$=9.10 Hz), 8.11 (d, 1H, –COCH, $J$=4.44 Hz), 9.93 (s, 1H, –COH). $^{13}$C NMR (75 MHz, $CDCl_3$): $\delta$ 14.06, 22.66, 25.94, 29.06, 29.32, 29.53, 29.55, 29.63, 31.89, 68.28, 97.66, 114.44, 127.41, 129.56, 130.79, 163.19, 176.49, 188.13.

### 4.7. 1-(4-Hexadecyloxyphenyl)-3-hydroxy-2-propen-1-one (3a; $n=16$)

Light yellow solids. $^1$H NMR (300 MHz, $CDCl_3$): $\delta$ 0.86 (t, 3H, $-CH_3$, $J$=6.65 Hz), 1.24–1.83 (m, 28H, $-CH_2$), 3.99 (t, 2H, $-OCH_2$, $J$=6.60 Hz), 6.13 (d, 1H, CH, $J$=4.40 Hz), 6.91 (d, 2H, Ar–H, $J$=8.80 Hz), 7.85 (d, 2H, Ar–H, $J$=8.80 Hz), 8.11 (d, 1H, –COCH, $J$=4.40 Hz), 9.93 (s, 1H, –COH). $^{13}$C NMR (75 MHz, $CDCl_3$): $\delta$ 14.09, 22.67, 25.95, 29.07, 29.34, 29.54, 29.56, 29.67, 31.91, 68.30, 97.67, 114.45, 127.42, 129.58, 130.81, 162.92, 163.20, 176.51, 188.14.

### 4.8. 4-Hexadecoxyphenyl butane-1,3-dione (3c; $n=16$)

Light yellow solid, yield 70%. $^1$H NMR ($CDCl_3$): $\delta$ 0.84 (t, $-CH_3$, 3H), 1.22–1.80 (m, $-CH_2$, 28H), 2.13 (s, $-COCH_3$, 3H), 3.97 (t, $-OCH_2$, 2H), 6.10 (s, –CCHCO, 1H), 6.92 (d, $-C_6H_4$, 2H), 7.81 (d, $-C_6H_4$, 2H), 16.30 (s, –OH, 1H). $^{13}$C NMR ($CDCl_3$): $\delta$ 14.07, 22.65, 25.24, 25.98, 29.37, 29.59, 29.69, 31.90, 68.05, 95.71, 114.58, 129.00, 130.18, 162.30, 183.97, 191.62.

### 4.9. 3-[4-Dodecyloxyphenyl]-1*H*-pyrazole (2a; $n=12$)

To he solution of 1-(4-dodecyloxyphenyl)-3-hydroxy-2-propen-1-one (3.00 g, 9.02 mmol) dissolved in 25 mL of THF/EtOH (1/1) was added 1.0 mL of dilute hydrochloric acid (3.0 M), and the solution was stirred for 5 min. To the solution was added hydrazine monohydrate (0.91 g) and the solution was refluxed for 12 h. The solids were filtered, and the products isolated as white solids were obtained after recrystallization from THF/EtOH. Yield 70–75%. White solid. $^1$H NMR (300 MHz, $CDCl_3$): $\delta$ 0.86 (t, 3H, $-CH_3$, $J$=6.72 Hz), 1.26–1.83 (m, 20H, $-CH_2$), 3.98 (t, 2H, $-OCH_2$, $J$=6.53 Hz), 6.55 (s, 1H, –CH═C), 6.96 (d, 2H, Ar–H, $J$=6.66 Hz), 7.63 (s, 1H, –C═CH), 7.68 (d, 2H, $-C_6H_4$, $J$=8.77 Hz). $^{13}$C NMR (75 MHz, $CDCl_3$): $\delta$ 14.09, 22.66, 26.03, 29.25, 29.33, 29.39, 29.58, 31.90, 68.12, 102.15, 114.86, 123.61, 127.21, 133.72, 148.23, 159.47.

### 4.10. 3-[4-Octyloxyphenyl]-1*H*-pyrazole (2a; $n=8$)

White solid. $^1$H NMR (300 MHz, $CDCl_3$): $\delta$ 0.89 (t, 3H, $-CH_3$, $J$=6.78 Hz), 1.28–1.82 (m, 12H, $-CH_2$), 3.96 (t, 2H, $-OCH_2$, $J$=6.57 Hz), 6.51 (d, 1H, –CH═C, $J$=2.19 Hz), 6.91 (d, 2H, Ar–H, $J$=8.77 Hz), 7.58 (d, 1H, –C═CH, $J$=2.22 Hz), 7.64 (d, 2H, Ar–H, $J$=8.80 Hz). $^{13}$C NMR (75 MHz, $CDCl_3$): $\delta$ 14.06, 22.63, 26.02, 29.22, 29.35, 68.01, 102.07, 114.81, 123.86, 127.15, 133.74, 148.28, 159.34.

### 4.11. 3-[4-Decyloxyphenyl]-1*H*-pyrazole (2a; $n=10$)

White solid. $^1$H NMR (300 MHz, $CDCl_3$): $\delta$ 0.87 (t, 3H, $-CH_3$, $J$=6.66 Hz), 1.26–1.82 (m, 16H, $-CH_2$), 3.96 (t, 2H, $-OCH_2$, $J$=6.56 Hz), 6.50 (s, 1H, –CH═C), 6.91 (d, 2H, Ar–H, $J$=8.74 Hz), 7.57 (s, 1H, –C═CH), 7.64 (d, 2H, Ar–H, $J$=8.71 Hz). $^{13}$C NMR (75 MHz, $CDCl_3$): $\delta$ 14.07, 22.65, 26.03, 29.25, 29.29, 29.39, 29.55, 31.87, 68.10, 102.06, 114.81, 123.93, 127.13, 133.74, 148.31, 159.32.

### 4.12. 3-[4-Tetradecyloxyphenyl]-1*H*-pyrazole (2a; $n=14$)

White solid. $^1$H NMR (300 MHz, $CDCl_3$): $\delta$ 0.86 (t, 3H, $-CH_3$, $J$=6.30 Hz), 1.24–1.79 (m, 24H, $-CH_2$), 3.97 (t, 2H, $-OCH_2$, $J$=6.35 Hz), 6.55 (s, 1H, –CH═C), 6.93 (d, 2H, Ar–H, $J$=6.54 Hz), 7.61 (s, 1H, –C═CH), 7.67 (d, 2H, Ar–H, $J$=8.65 Hz). $^{13}$C NMR (75 MHz, $CDCl_3$): $\delta$ 14.09, 22.67, 26.03, 29.24, 29.34, 29.40, 29.59, 31.91, 68.13, 102.25, 114.88, 123.44, 127.26, 133.75, 145.12, 159.52.

### 4.13. 3-[4-Hexadecyloxyphenyl]-1*H*-pyrazole (2a; $n=16$)

White solid. $^1$H NMR (300 MHz, $CDCl_3$): $\delta$ 0.86 (t, 3H, $-CH_3$, $J$=6.69 Hz), 1.24–1.83 (m, 28H, $-CH_2$), 3.97 (t, 2H, $-OCH_2$, $J$=6.65 Hz), 6.54 (s, 1H, –CH═C), 6.93 (d, 2H, Ar–H, $J$=8.74 Hz), 7.62 (s, 1H, –C═CH), 7.67 (d, 2H, Ar–H, $J$=8.47 Hz). $^{13}$C NMR (75 MHz, $CDCl_3$): $\delta$ 14.08, 22.66, 26.03, 29.25, 29.33, 29.29, 29.58, 29.67, 31.90, 68.11, 102.14, 114.82, 123.85, 127.15, 133.85, 148.36, 159.36.

### 4.14. 3-[3,4-Dihexadecyloxyphenyl]-1*H*-pyrazole (2b; $n=16$)

White solid. $^1$H NMR (300 MHz, $CDCl_3$): $\delta$ 0.86 (t, 3H, $-CH_3$, $J$=6.71 Hz), 1.17–1.85 (m, 56H, $-CH_2$), 4.01 (t, 2H, $-OCH_2$, $J$=6.63 Hz), 6.50 (d, 1H, –CH═C–N, $J$=2.04 Hz), 6.87 (d, 1H, Ar–H, $J$=8.31 Hz), 7.20 (d, 1H, Ar–H, $J$=1.98 Hz), 7.29 (d, 1H, Ar–H, $J$=1.98 Hz), 7.56 (d, 1H, ═CHN, $J$=2.01 Hz). $^{13}$C NMR (75 MHz, $CDCl_3$): $\delta$ 14.08, 22.67, 26.04, 29.35, 29.44, 29.65, 29.70, 31.91, 69.37, 102.21, 111.57, 113.97, 118.53, 124.96, 133.26, 148.94, 149.36, 149.43.

### 4.15. 3-(4-(Hexadecyloxy)phenyl)-5-methyl-1*H*-pyrazole (2c; $n=16$)

White solid, yield 83%. $^1$H NMR (300 MHz, $CDCl_3$): $\delta$ 0.84 (t, $-CH_3$, 3H), 1.19–1.79 (m, $CH_2$, 28H), 2.37 (s, $-CNCH_3$, 3H), 3.96 (t, $-OCH_2$, 2H), 6.33 (s, –CNCH, 1H), 6.86 (d, $-C_6H_4$, 2H), 7.66 (d, $-C_6H_4$, 2H). $^{13}$C NMR ($CDCl_3$): $\delta$ 12.04, 14.15, 22.72, 26.05, 29.29, 29.46, 29.63, 31.82, 68.10, 102.89, 114.96, 125.08, 126.98, 142.96, 149.68, 159.62.

### 4.16. Copper complexes 3-[4-alkoxyphenyl]-1*H*-pyrazoles (1a; $n=8, 10, 12, 14, 16$)

The mixture of 3-[4-(dodecyloxy)phenyl]-1*H*-pyrazole (0.3 g, 0.304 mmol) and copper(II) chloride dehydrate (0.052 g, 0.304 mmol) was refluxed in ethanol for 3 h. The solids were filtered. The products isolated as bright yellow-greenish solids were obtained after recrystallization from THF/ethyl acetate. Yield 87–90%. Anal. Calcd. for **1a** ($n$ = 8) $C_{34}H_{48}O_2N_4CuCl_2$: C, 60.12; H, 7.12. Found: C, 60.06; H, 7.11. **1a** ($n$ = 10) $C_{38}H_{56}O_2N_4CuCl_2$: C, 62.07; H, 7.68. Found: C, 62.19; H, 7.76. **1a** ($n$ = 12) $C_{42}H_{64}O_2N_4CuCl_2$: C, 63.74; H, 8.15. Found: C, 63.80 H, 8.33. **1a** ($n$ = 14): $C_{46}H_{72}O_2N_4CuCl_2$: C, 65.19; H, 8.56. Found: C, 64.87; H, 8.44. **1a** ($n$ = 16) $C_{50}H_{80}O_2N_4CuCl_2$: C, 66.46; H, 8.92. Found: C, 66.41; H, 8.91.

## Acknowledgements

We thank the National Science Council of Taiwan (NSC 97-2738-M-008-001 and NSC 98-2752-M-008-001-PAE) and also Display Technology Center and Active Device Technology Dept., EOL/Industrial Technology Research Institute of Taiwan, ROC (ITRI 98-B-08-8351AA5140) in generous support of this work.

## References and notes

1. (a) Trofimenko, S. *Chem. Rev.* **1972**, *72*, 497–509; (b) Trofimenko, S. *Prog. Inorg. Chem.* **1986**, *34*, 115–210; (c) Niedenzu, K.; Trofimenko, S. *Top. Curr. Chem.* **1986**, *131*, 1–37.
2. (a) La Monica, G.; Ardizzoia, G. A. *Prog. Inorg. Chem.* **1997**, *46*, 151–238; (b) Rasika Dias, H. V.; Diybalanage, H. V. K.; Eldabaja, M. G.; Elbjeirami, O.; Rawashdeh-Omary, M. A.; Omary, M. A. *J. Am. Chem. Soc.* **2005**, *127*, 7489–7501; (c) Rasika Dias, H. V.; Palehepitiya Gamage, C. S.; Keltner, J.; Diyabalanage, H. V. K.; Omari, I.; Eyobo, Y.; Dias, N. R.; Roehr, N.; McKinney, L.; Poth, T. *Inorg. Chem.* **2007**, *46*, 2979–2987.
3. (a) Paraschiv, I.; Giesbers, M.; Lagen, B. V.; Grozema, F. C.; Abellon, R. D.; Siebbeles; Antonius, L. D. A.; Marcelis, T. M.; Zuilhof, H.; Sudhölter, E. J. R. *J. Am. Chem. Soc.* **2006**, *18*, 968–974; (b) Wang, Y. J.; Song, J. H.; Lin, Y. S.; Lin, C.; Sheu, H. S.; Lee, G. H.; Lai, C. K. *Chem. Commun.* **2006**, 4912–4914; (c) Ziessel, R.; Pickaert, G.; Camerel, F.; Donnio, B.; Guillon, D.; Cesario, M.; Prange, T. *J. Am. Chem. Soc.* **2004**, *126*, 12403–12413.

4. (a) Chen, Y.; Harrison, W. T. A.; Imrie, C. T.; Ryder, K. S. *J. Mater. Chem.* **2002**, *12*, 579–585; (b) Barberá, J.; Gimnénez, R.; Serrano, J. L. *Chem. Mater.* **2000**, *12*, 481–489.
5. Barbara, J.; Cativiela, C.; Serrano, J. L. *Liq. Cryst.* **1992**, *11*, 887–897.
6. Kishiura, A.; Yamashita, T.; Aida, T. *J. Am. Chem. Soc.* **2005**, *127*, 179–183.
7. (a) Giménez, R.; Elduque, A.; López, J. A.; Barberá, J.; Cavero, E.; Lantero, I.; Oro, L. A.; Serrano, J. L. *Inorg. Chem.* **2006**, *45*, 10363–10370; (b) Torralba, M. C.; Cano, M.; Campo, j. A.; Heras, J. V.; Pinilla, E.; Torres, M. R. *J. Organomet. Chem.* **2002**, *654*, 150–161; (c) Torralba, M. C.; Cano, M.; Campo, J. A.; Heras, J. V.; Pinilla, E.; Torres, M. R. *J. Organomet. Chem.* **2001**, *633*, 91–104; (d) Barberá, J.; Elduque, A.; Giménez, R.; Lahoz, F. L.; López, J. A.; Oro, L. A.; Serrano, J. L.; Villacampa, B.; Villalba, J. *Inorg. Chem.* **1999**, *38*, 3085–3092.
8. Chou, S. Y.; Chen, C. J.; Tsai, S. L.; Sheu, H. S.; Lee, G. H.; Lai, C. K. *Tetrahedron* **2009**, *65*, 1130–1139.
9. (a) Torralba, M. C.; Campo, J. A.; Heras, J. V.; Bruce, D. W.; Cano, C. *Dalton Trans.* **2006**, 3918–3926; (b) Torralba, M. C.; Cano, M.; Campo, J. A.; Heras, J. V.; Pinilla, E.; Torres, M. R. *Inorg. Chem. Commun.* **2006**, *9*, 1271–1275; (c) Torralba, M. C.; Cano, M.; Campo, J. A.; Heras, J. V.; Pinilla, E.; Torres, M. R. *J. Organomet. Chem.* **2006**, *691*, 765–778; (d) Torralba, M. C.; Cano, C.; Gómez, S.; Campo, J. A.; Heras, J. V.; Perles, J.; uiz-Valero, C. *J. Organomet. Chem.* **2003**, *682*, 26–34; (e) Mayoral, M. J.; Torralba, M. C.; Cano, M.; Campo, J. A.; Heras, J. V. *Inorg. Chem. Commun.* **2003**, *6*, 626–629; (f) Torralba, M. C.; Cano, C.; Campo, J. A.; Heras, J. V.; Pinilla, E.; Torres, M. R. *Inorg. Chem. Commun.* **2002**, *5*, 887–890; (g) Torralba, M. C.; Cano, M.; Campo, J. A.; Heras, J. V.; Pinilla, E. *Z. Kristallogr.- New Cryst. Struct.* **2005**, *220*, 615–616.
10. Lin, H. D.; Lai, C. K. *Dalton Trans.* **2001**, 2383–2387.
11. (a) Rasika Dias, H. V.; Diyabalanage, H. V. K. *Polyhedron* **2006**, *15*, 1655–1661; (b) Mohamed, A. A.; Pérez, L. M.; Fackler, J. P., Jr. *Inorg. Chim. Acta* **2005**, *358*, 1657–1662; (c) Kim, S. J.; Kang, S. H.; Park, K. M.; Kim, H.; Zin, W. C.; Choi, M. G.; Kim, K. *Chem. Mater.* **1998**, *10*, 1889–1893; (d) Barberá, J.; Elduque, A.; Giménez, R.; Lahoz, F. L.; López, J. A.; Oro, L. A.; Serrano, J. L. *Inorg. Chem.* **1998**, *37*, 2960–2967; (e) Mayoral, M. J.; Ovejero, P.; Campo, J. A.; Heras, J. V.; Pinilla, E.; Torres, M. R.; Lodeiro, C.; Cano, M. *Dalton Trans.* **2008**, 6912–6924.
12. (a) Cavero, E.; Uriel, S.; Romero, P.; Serrano, J. L.; Gimnez, R. *J. Am. Chem. Soc.* **2008**, *129*, 11608–11618; (b) Giménez, R.; Manrique, A. B.; Uriel, S.; Barberá, J.; Serrano, J. L. *Chem. Commun.* **2004**, 2064–2065.
13. Shen, W. C.; Wang, Y. J.; Cheng, K. L.; Lee, G. H.; Lai, C. K. *Tetrahedron* **2006**, *62*, 8035–8044.
14. (a) Lai, C. K.; Pang, Y. S.; Tsai, C. H. *J. Mater. Chem.* **1998**, *8*, 2605–2610; (b) Yang, C. D.; Pang, Y. S.; Lai, C. K. *Liq. Cryst.* **2001**, *28*, 191–195.
15. Lai, C. K.; Lin, R.; Lu, M. Y.; Kao, K. C. *J. Chem. Soc., Dalton Trans.* **1998**, 1857–1862.
16. (a) Barberá, J.; Giménez, R.; Marcos, M.; Serrano, J. L.; Alonso, P. J.; Martínez, J. I. *Chem. Mater.* **2003**, *15*, 958–964; (b) Lin, R.; Tsai, C. H.; Chao, M. Q.; Lai, C. K. *J. Mater. Chem.* **2001**, *11*, 359–363.